



The Open Civil Engineering Journal

Content list available at: www.benthamopen.com/TOCIEJ/

DOI: 10.2174/1874149501610010373



RESEARCH ARTICLE

Research on Seismic Performance of Reinforced Concrete Frame with Unequal Span Under Low Cyclic Reversed Loading

Wang Lai^{1,*}, Xuan Wei¹, Feng Ning-ning², Cong Shuping¹, Liu Feng¹ and Gao Qiumei¹¹Shandong Provincial Key Laboratory of Civil Engineering Disaster Prevention and Mitigation, Shandong University of Science and Technology, Qingdao 266590, China²College of Civil and Transportation Engineering, Hohai University, Nanjing 210098, China

Received: November 6, 2015

Revised: January 27, 2016

Accepted: February 25, 2016

Abstract: In order to investigate the seismic performance of reinforced concrete frame with unequal span, a specimen was tested under low-cyclic loading and the seismic performance of this frame was analyzed based on fiber element method using software OpenSees. Hysteretic curves, skeleton curves, ductility, stiffness degradation and energy dissipating capacity of the frame are compared and analyzed. The experimental and simulate results demonstrate that this frame has a poor seismic performance. Thus, it is suggested that the seismic strengthening criteria of unequal-span frame structure should be raised and the existing buildings of this structure should be retrofitted.

Keywords: Ductility, energy dissipation, hysteresis analysis, low cyclic loading test, OpenSees numerical simulation, reinforced concrete frame, skeleton curve, stiffness degradation.

1. INTRODUCTION

Many school buildings including those of reinforced concrete (RC) frame structural system have suffered severe damage during earthquakes. The seismic performance of RC frames has been extensively studied by a number of experts. Mpampatsikos *et al.* [1] assess the seismic behavior of two existing reinforced concrete frames according to Eurocode 8 and Italian seismic code, by checking the ductility mechanisms and brittle mechanisms of those structures. Bilgin [2] believes the structural system of school buildings in Turkey has poor seismic bearing capacity and proposes to strengthen them by adding shear wall in longitudinal and transverse direction, through evaluating the seismic performance of a four-storey reinforced concrete frame. Shrestha *et al.* [3] investigate the vulnerabilities of 58 buildings of 19 school in Aceh, Indonesia by onsite test and partially destructive test, and compare the cost-effect of retrofitting approach and rebuilt approach.

After Wenchuan Earthquake, seismic damages of RC frames structural buildings [4] are investigated. A number of systematic researches in China have been carried out on the basic seismic performances of frame structures and failure characteristics from the perspectives of frame beams [5, 6], frame columns [7, 8], frame joints [9, 10] and the whole structures [11 - 15].

Xuankou School building [16 - 19] is a typical RC frame structure with two unequal spans, which is a popular structure in Primary and middle school in China. Please refer to Fig. (1) for the destroyed Xuankou School building.

In order to evaluate seismic performance of the structure such as Xuankou School building, this study examines a 1/2 scale two-storey and two-bay RC frame designed in accordance with Chinese code for seismic design of buildings (GB50011-2010), adopting pseudo-static approach.

* Address to correspondence to this author at Shandong Provincial Key Laboratory of Civil Engineering Disaster Prevention and Mitigation, Shandong University of Science and Technology Qingdao 266590, China; Tel: (86)13789879265; E-mail: wlkdtxjy@sina.com

Based on the assumption of small deformation and plane section, fiber element method [20, 21] is widely used in numerical analysis and has been verified to be effective to assess nonlinear response of braced frames [22 - 26] and evaluating the capacity of precast-prestressed slabs [27, 28]. This method is suitable to different sections since it discretizes the cross-section into fibers. Furthermore, it is relatively more accurate as the element section force deformation relation is derived by integration of the stress-strain relation of the fibers.

Both the experimental results and numerical analysis using software OpenSees verify this structure has poor seismic performance.



Fig. (1). Collapse of Xuankou Middle School building.

2. EXPERIMENTAL PROGRAM

2.1. Test Specimen

The test specimen is two-storey and two-bay RC frame structure, with span lengths of 3.0m and 1.2m. The frame is at 1/2 scale with storey height of 1.5m and total height of 3.6m. The cross sections of the beams and columns are 150mm by 250mm and 200mm by 250mm, while the ground beam is 350mm by 400mm. The compressive cube strength of the concrete, based on the average value obtained from coupon tests, is 23.8MPa. The longitudinal reinforcements in beams and columns employ HRB335, with diameter of 16mm, yield strength of 425MPa and ultimate strength of 565MPa, while the stirrups in beams and columns apply HPB235, with diameter of 8mm, yield strength of 305MPa, ultimate strength of 445MPa. The dimensions and the reinforcements of the frame are depicted in Fig. (2).

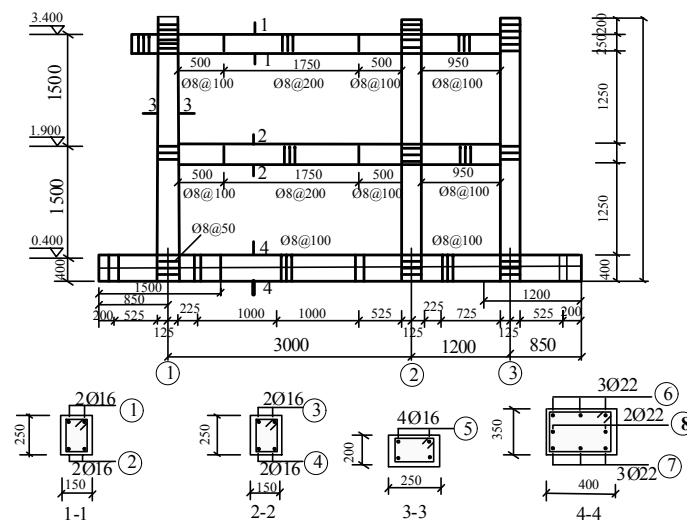


Fig. (2). Dimensions and reinforcement detail.

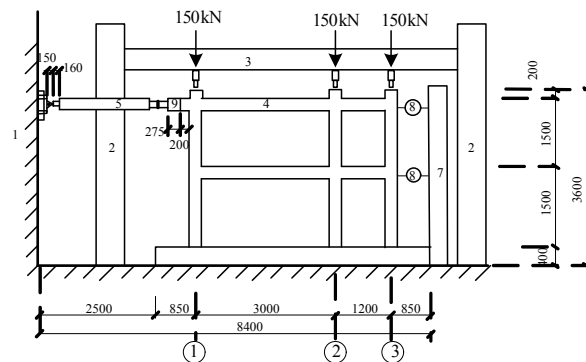
2.2. Test Setup and Instrumentation

The specimen is subjected to quasi-static cyclic loading on beam end of the second floor. As shown in Fig. (3), the specimen is bolted to the rigid floor through the six holes in the base girder. Constant vertical loads of 150kN (to simulate gravity load to this specimen when axial load ratio is 0.25) are applied to the three column tops by three mechanical jacks. The mechanical jacks are connected to the steel beam by roller bearings, which maintain free horizontal displacement of the frame under vertical loads and horizontal loadings. The horizontal cyclic loadings are imposed by a servo-hydraulic actuator made by Beijing Fluid Control System Corp. Loading of the specimen is illustrated in Fig. (4). The test instruments are preloaded to ensure the stability at initial stage. The application of simulation cyclic loads is based on a hybrid force/displacement control. Before yield of specimen, the test is at force control stage. The specimen is loaded one cycle at each force level with loading value of 20kN. When the specimen yielded, the test reached the displacement control stage. The specimen is loaded two cycles at every displacement level while the loading value is integral multiples of yield displacement.

When the displacement reaches $4\Delta_y$ and the current capacity of the specimen decreases to 85% of maximum bearing capacity.



Fig. (3a). Test setup.



- 1 reaction wall 2 steel column 3 steel beam 4 specimen
- 5 actuator 6 mechanical jack 7 steel column of displacement meters 8 displacement meters 9 connector

Fig. (3b). Test setup.

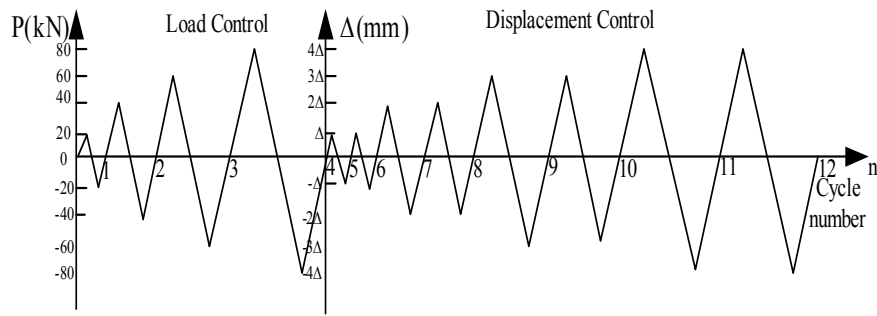
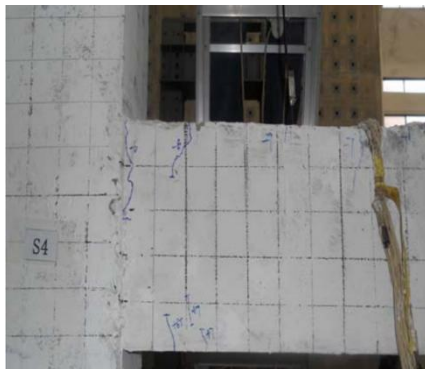


Fig. (4). Loading program.

2.3. Test Description

The failure pattern is illustrated in Fig. (5). In the area of 5cm-6cm away from beam end, some diagonal cracks in length ranged from 7cm to 12cm appear at first. Then the cracks extend to the mid-span of the beam and some cracks are observed in the area of 10cm-38cm away from the beam end. When the loading reaches -60kN, an 8cm long crack appears at bottom of the column on the first floor. When the loading reaches 70kN, some cracks appear in the area 28-36cm away from the top of columns. At the stage of displacement control, the cracks of the columns extend further and even run through the whole cross-sections of columns, while the longitudinal reinforcements of beams begin to yield. After the yield, the cross diagonal cracks at the joint zone grow, and the specimen reaches splitting failure in the end. At the later stage of the loading, the “zi, zi” sound comes from the inside of the frame, the concrete peels partially at the beam end, bottom of the column and joints region. When the current capacity of the specimen decreases to 85% of maximum bearing capacity, the specimen reaches its ultimate state.



(a) Cracks at beam end



(b) Cracks at column bottom



(c) Cracks at joints zone

Fig. (5). Specimen failure pattern.

2.4. Numerical Simulation

The reinforcement concrete frame is simulated using software OpenSees based on fiber element method, adopting nonlinear beam-column elements with 6 integrate points. The beam and column elements are defined respectively for the different confinement of stirrups. The data would be more accurate and ideal if the plastic hinge element is considered. To avoid too complicated numerical model the plastic hinge model was not added in this study.

2.4.1. Strain-Stress Relationship of Steel

A uniaxial Giuffre-Menegotto-Pinto steel material object with isotropic strain hardening is taken into consideration in the steel material named Steel02 in OpenSees. The yield strength and modulus of steel are obtained from test results and parameters to control the transition from elastic to plastic branches named R0, CR1 and CR2 are 18, 0.925 and 0.15. The stress-strain curve of steel is shown as Fig. (6a).

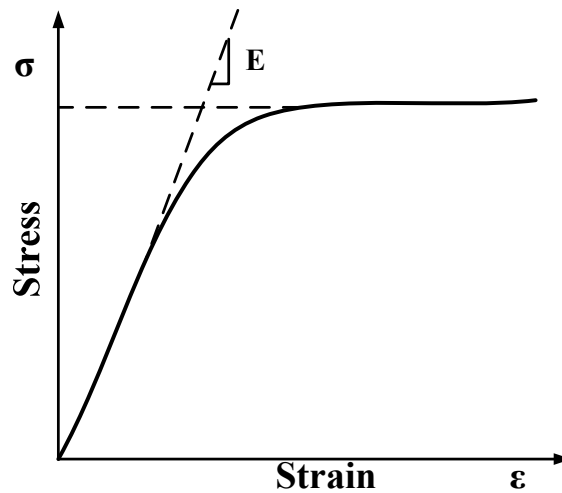


Fig. (6a). Steel stress-strain curve.

2.4.2. Stress-Strain Relationship of Concrete

The Concrete02 material object in OpenSees software is employed in this concrete frame. The eps_{co} is concrete strain at the maximum stress point, f_{pc} is concrete compressive cylinder strength, eps_U is concrete strain at the crushing strength, f_{pcu} is concrete crushing strength, λ is the ratio between unloading slope at crushing strain and initial slope, f_t represents concrete tension strength and E_{ts} is tension softening stiffness. In this model, the initial elastic modulus E_c is got from the test, which value is $2.42 \times 10^5 \text{ N/mm}^2$. The stress-strain curve of concrete is illustrated in Fig. (6b).

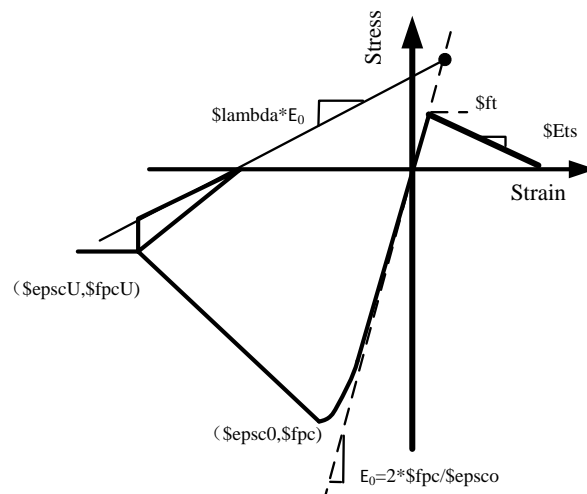


Fig. (6b). Steel stress-strain curve.

The stress-strain relationships of covered concrete and core concrete (confinement of stirrups) are considered as follows:

(1) The cylinder strength f_c^l is taken as maximum strength of covered concrete, its value is 0.76 times cubic compressive strength according to core for design of concrete structures [29], the strain at maximum stress point is taken as $epsco = 2 \times f_c^l / 2E_c$ and the values of stress and strain at crushing strength point are as follows: $epsU = -0.0038$ $f_{pcu} = 0.2f_c^l$ $\lambda = 0.1$ the tension strength is, $f_t = 0.1 f_c^l$ and the tension elastic modulus is $E_{ts} = 0.1 E_c$.

(2) The values of core concrete are calculated in accordance with Mander's method [30], which are f_{pc} , $epsco$ at maximum stress point and f_{pcu} , $epsU$ at crushing strength point. As the configurations of stirrups are different in the columns, ends and mid-span of the beams, confinement on different core concrete parts varies. In accordance with the confinement of stirrups, the core concrete elements of beam and column can be divided into three elements:

1. Column elements confined by stirrups;
2. Beam elements confined by stirrups;
3. Covered concrete elements.

The core concrete element types are illustrated in Fig. (7).

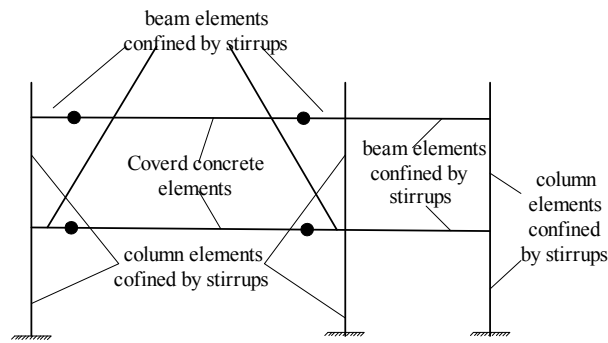


Fig. (7). The core concrete elements of beams and columns.

3. RESULTS AND DISCUSSION

3.1. Hysteretic Curve

The hysteretic curves of the horizontal load on the specimen and the displacement on the top of the second floor are shown in Fig. (8). At the beginning of loading, the hysteretic curve is almost linear and the slope is quite steep. With the increase of loads, the specimen starts to crack; when the specimen reaches the yield point, the hysteretic loop becomes plumper. When the loading is under displacement control, the curve becomes smoother; the stiffness of specimen is degraded gradually, and the hysteretic loop begins to present pinch phenomenon. When the components have obvious slip, the specimen tends to fail and the hysteretic loop is on reverse S-shape.

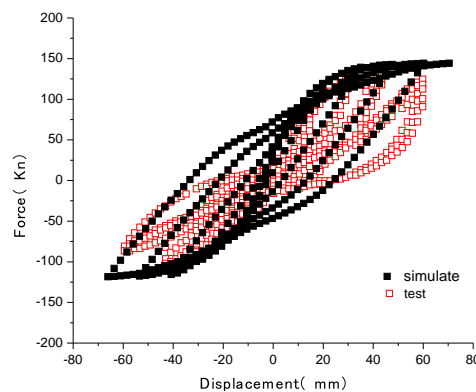


Fig. (8). Hysteretic curve.

There is a little deviation between the experimental data and numerical data in Fig. (8). The two results would be more consistent [31] if the factors such as plastic hinge element, cracks and bond-slip were taken into consideration.

3.2. Skeleton Curve

The skeleton curve of the specimen is depicted in Fig. (9). It can be observed that at the beginning of loading, the curve is linear in state and the specimen is in elastic stage. With the increase of the loading, the specimen enters the plastic stage, the cracks grow gradually and the stiffness decreases. Therefore, the slope of skeleton decreases gradually, and tends to X axis direction. When the loading reaches 80kN, the slope of skeleton decreases tremendously, the curvature speeds up its decrease rate. The curve slope becomes negative after the maximum load point, while the load decreases gradually with the increase of displacement until it reaches the ultimate load. The structural bearing capacity decreases rapidly with cracks growing gradually, following the increase of loading during test process. On the contrary, structural bearing capacity decreases slowly during the simulate process. It is because that numerical model is ideal without taking cracks [32, 33] into account. While, in reality the cracks would significantly influence the strength, stiffness, ductility and other parameters of concrete structures.

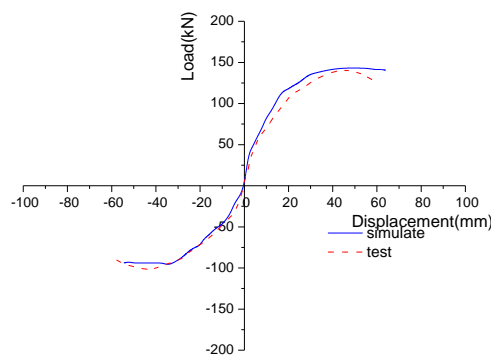


Fig. (9). Skeleton curve.

Table 1. Test results and ductility factor.

Specimen	Direction	Test	Model
Yield load	positive	94.25kN	106.5kN
	negative	66.04kN	94.8kN
Yield displacement	positive	19.69mm	106.5mm
	negative	19.05mm	94.8mm
Maximum load	positive	142.4kN	19.98 kN
	negative	103.8 kN	18.72 kN
Maximum displacement	positive	44.7 mm	45.5mm
	negative	44.2mm	36.8mm
Ultimate Load	positive	120.7kN	140.3 kN
	negative	88.0 kN	93.9 kN
Ultimate displacement	positive	61.2mm	64.1mm
	negative	57.2mm	54.5mm
Ductility factor	positive	3.1	3.2
	negative	3.0	2.9

3.3. Ductility Analysis

Yield load and displacement are calculated using general yield moment method, and maximum load and displacement, ultimate load and displacement of the specimen generated from hysteretic curve and skeleton curve offer data for the calculation of ductility coefficient. As shown in the experimental results and ductility coefficient of Table 1, the load in the positive direction is higher than that in reverse direction, which is caused by the damaged accumulation of the frame. Although the ductility coefficient of the frame is higher than the coefficient of 3.0 in normal cases, this relatively low value indicates the poor ductility performance. It also demonstrates that the reinforced frame is

vulnerable to severe destruction when subjected to external load.

3.4. Stiffness Degradation Curve

Stiffness degradation curve of the specimen is shown in Fig. (10). It can be observed that the secant stiffness decreases with the increase of displacement, which indicates the trend of stiffness degradation of the frame. Secant stiffness drops suddenly from 10kN/mm to 6kN/mm, which illustrates the rapid stiffness degradation caused by the appearance of new cracks and growth of old ones. The specimen has the maximum stiffness at the early stage, and then it degrades gradually with the growth of cracks and accumulation of internal damage. When the loading gets 80kN and corresponding secant stiffness reaches 4.13, the frame begins to yield, the primary cracks are formed and the stiffness degradation becomes relatively stable. After that, the stiffness degradation ratio becomes slower until the specimen reaches its ultimate state.

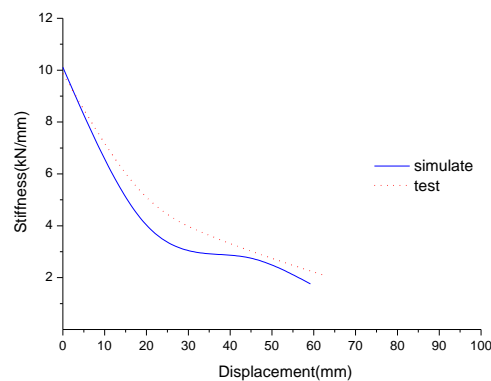


Fig. (10). Stiffness degradation curve.

3.5. Energy Dissipation Curve

The equivalent viscous damping factor [34] is calculated based on the areas of hysteretic loop and corresponding triangle. The relation curve of equivalent viscous damping coefficient and corresponding displacement is depicted in Fig. (11). As can be seen in Fig. (11), the equivalent viscous damping factor grows with the increase of displacement, but the ratio of increase has little change. The increase of equivalent viscous damping coefficient proves a gradual growth of energy dissipation of specimen, while the minor change in the ratio of increase indicates that the frame has low energy dissipation capacity, which corresponds to the pinching phenomenon of hysteretic loop in Fig. (9).

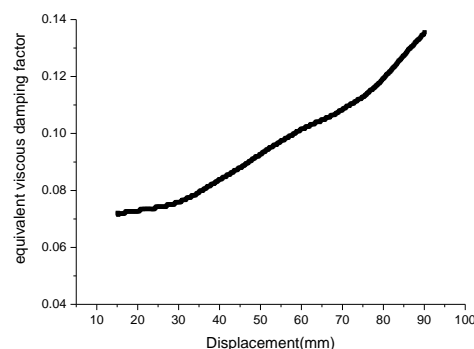


Fig. (11). The graph of equivalent viscous damping coefficient.

Even though the equivalent viscous damping factor is slightly overestimated as stated by Brunesi [35], it correctly reflects energy dissipation trend of the structure. The small area of hysteretic loop confirms that the RC frame has poor energy dissipation capacity.

CONCLUSION

Focused on the seismic performance of two-story and two-span RC frame under low cyclic loading, the following conclusions can be drawn from the numerical analysis and experimental results of the research:

1. The reverse S-shape of hysteretic curve of the test results demonstrates that the frame has a low energy dissipation capacity. This is because the stiffness degraded severely when the concrete cracks, the longitudinal reinforcement yields, the cracks grow significantly at the bottoms of three columns, and the variation of displacement exceeds the variation of loads, and the components slip tremendously.
2. The data of yield load and displacement, maximum load and displacement, ultimate load and displacement from hysteretic curve show the difference between positive and reverse loading, while the difference of data is mainly caused by damage accumulation during loading on the frame. The displacement ductility coefficient of approximately 3.0 demonstrates that the frame has low deformability.
3. The frame stiffness degradation is remarkable before the main crack formed. After that, the secant stiffness decreases with the increase of displacement but the ratio of decrease is slow, which shows that the frame stiffness degradation grows slower. The frame energy dissipation curve increases with the increase of displacement, which confirms that the energy dissipation of the specimen is becoming stronger. Because of the pinching phenomenon of hysteretic loop, the ratio of energy dissipation increase is small, which indicates that the frame has low energy dissipation capacity.
4. The ideal model is used in numerical simulation without taking into account the impacts of cracks in the frame, reinforced slip and other factors, thus there are some deviations between simulate and experimental results.
5. Although the RC unequal-span frame is widely used in primary and middle school buildings in China, its seismic performance is relatively poor. Therefore, it is necessary to raise the seismic strengthening criteria of unequal-span frame structure and to retrofit the existing buildings of this structure.

CONFLICT OF INTEREST

The authors confirm that this article content has no conflict of interest.

ACKNOWLEDGEMENTS

This study was financially supported by National Natural Foundation of China in 2012(No.51178259) and Postgraduate innovation fund of Shandong University Science and Technology (No. YC150328).

REFERENCES

- [1] V. Mpampatsikos, R. Nascimbene, and L. Petrini, "A critical review of the RC frame existing building assessment procedure according to Eurocode 8 and Italian seismic code", *Journal of Earthquake Engineering*, vol. 12, pp. 52-82, 2008. [<http://dx.doi.org/10.1080/13632460801925020>]
- [2] H. Bilgin, "Seismic performance evaluation of an existing school building in Turkey", In: *9th International Congress on Advances in Civil Engineering*, Karadeniz Technical University: Trabzon, Turkey, 2010.
- [3] H.D. Shrestha, R. Yatabe, N.P. Bhandary, and J. Subedi, "Vulnerability assessment and retrofitting of existing school buildings: a case study of Aceh", *International Journal of Disaster Resilience in the Built Environment*, vol. 3, pp. 52-65, 2012. [<http://dx.doi.org/10.1108/17595901211201132>]
- [4] Y. Lieping, L. Xinzheng, Z. Shiyang, and L. Yi, "Seismic collapse resistance of RC frame structural -- case studies on seismic damages of several RC frames under extreme ground motion in Wenchuan earthquake", *Journal of Building Structures*, vol. 30, pp. 67-76, 2009.
- [5] G. WU, L. AN, and Z. LU, "Experimental study on bending properties of reinforced concrete beams strengthened with carbon fiber sheets", *Building Structure*, vol. 30, pp. 6-10, 2000.
- [6] W. Bo, W. Weijun, and Z. Zhengxian, "An experimental study on reinforced concrete frame beams strengthened with carbon fiber sheets under cyclic loading", *World Earthquake Engineering*, vol. 19, pp. 62-69, 2003.
- [7] X. Jianyun, W. Jiansheng, and K. Suzuki, "Behaviour of reinforced concrete columns under cyclic lateral load", *China Civil Engineering Journal*, vol. 24, pp. 57-70, 1991.
- [8] G. Xiuli, "Experimental Investigation and Damage Model Research of RC Frame Column". Master's degree, Hefei University of Technology: China, 2009.
- [9] L. Xilin, G. Zixiong, and W. Yayong, "Experimental study on seismic behavior of beam-column subassemblages in RC frame", *Journal of Building Structures*, vol. 22, pp. 2-7, 2001.
- [10] W. Yulei, "Experimental Study on the Behaviors of Exterior Joints of RC Frame Under Low Cyclic Loading", Master's degree, Harbin

Institute of Technology, China, 2010.

- [11] Z. Yicun, R. Fudong, and T. Jiahua, "An experimental study on the elastoplastic behavior of Two-Bay Two-Storey reinforced concrete frames", *Journal of Building Structures*, vol. 2, pp. 34-41, 1981.
- [12] X. Weichen, and H. Xiang, "Seismic performance of four-story two-bay HPC frame", *Journal of Building Structures*, vol. 28, pp. 69-79, 2007.
- [13] W. Lai, "T. WANG, and J. QI, "Experimental and theoretical study on hysteretic behavior of concrete-filled rectangular steel tubular frame", *Tianjin Daxue Xuebao*, vol. 38, pp. 41-46, 2005.
- [14] Z. Xuan, and Z. Deyuan, "Experimental analysis of 3-story RC frame structures under cyclic load reversals", *Sichuan Building Science*, vol. 31, pp. 7-11, 2005.
- [15] X. Yunfei, H. Qingchang, and C. Yufeng, "The experimental study of the behavior of a Two-Bay Three-Story RC frame under cyclic loading", *Journal of Building Structures*, vol. 7, pp. 1-16, 1986.
- [16] J. Huan, and D. Junwu, "Study on seismic behavior of side corridor RC frame school buildings", *China Civil Engineering Journal*, vol. 46, pp. 71-77, 2013.
- [17] M. Yuhu, L. Xinzheng, Y. Lieping, T. Daiyuan, and L. Yi, "Seismic damage simulation and analysis of typical RC frame of Xuankou school", *Engineering Mechanics*, vol. 28, pp. 71-77, 2011.
- [18] Y. Weisong, "*Experimental Study on Collapse Mechanism of Multi-storey RC Frame School Buildings*", Phd. Thesis, Institute of Engineering, Earthquake Administration, China, 2015.
- [19] Y. LiePing, L. Yi, and P. Peng, "Seismic damage of building structure of XuanKou Middle school in YingXiu town", *Buildings Structure*, pp. 54-57, 2009.
- [20] F. Taucer, E. Spacone, and F.C. Filippou, "*A Fiber Beam-Column Element for Seismic Response Analysis of Reinforced Concrete Structures*", Report No. UCB/EERC-91/17, Earthquake Engineering Research Center, College of Engineering, University of California, Berkeley, 1991.
- [21] E. Spacone, F.C. Filippou, and F.F. Taucer, "Fibre beam-column model for non-linear analysis of R/C frames: Part I. Formulation", *Earthquake Engineering and Structural Dynamics*, vol. 25, pp. 711-726, 1996.
[[http://dx.doi.org/10.1002/\(SICI\)1096-9845\(199607\)25:7<711::AID-EQE576>3.0.CO;2-9](http://dx.doi.org/10.1002/(SICI)1096-9845(199607)25:7<711::AID-EQE576>3.0.CO;2-9)]
- [22] E. Fagà, G. Rassati, and R. Nascimbene, "Seismic design of elevated steel tanks with concentrically braced supporting frames", In: *Structures Congress 2012, ASCE*, 2012, pp. 1473-1484.
[<http://dx.doi.org/10.1061/9780784412367.131>]
- [23] K. Wijesundara, G. Rassathi, R. Nascimbene, and D. Bolognini, "Seismic performance of brace-beam-column connections in concentrically braced frames", In: *Structural Congress, ASCE*, 2010, pp. 930-942.
[[http://dx.doi.org/10.1061/41130\(369\)85](http://dx.doi.org/10.1061/41130(369)85)]
- [24] K. Wijesundara, R. Nascimbene, and G. Rassati, "Modeling of different bracing configurations in multi-storey concentrically braced frames using a fiber-beam based approach", *Journal of Constructional Steel Research*, vol. 101, pp. 426-436, 2014.
[<http://dx.doi.org/10.1016/j.jcsr.2014.06.009>]
- [25] E. Brunesi, R. Nascimbene, and G. Rassati, "Response of partially-restrained bolted beam-to-column connections under cyclic loads", *Journal of Constructional Steel Research*, vol. 97, pp. 24-38, 2014.
[<http://dx.doi.org/10.1016/j.jcsr.2014.01.014>]
- [26] E. Brunesi, R. Nascimbene, and G. Rassati, "Seismic response of MRFs with partially-restrained bolted beam-to-column connections through FE analyses", *Journal of Constructional Steel Research*, vol. 107, pp. 37-49, 2015.
[<http://dx.doi.org/10.1016/j.jcsr.2014.12.022>]
- [27] E. Brunesi, D. Bolognini, and R. Nascimbene, "Evaluation of the shear capacity of precast-prestressed hollow core slabs: numerical and experimental comparisons", *Materials and Structures*, vol. 48, pp. 1503-1521, 2014.
[<http://dx.doi.org/10.1617/s11527-014-0250-6>]
- [28] E. Brunesi, and R. Nascimbene, "Numerical web-shear strength assessment of precast prestressed hollow core slab units", *Engineering Structures*, vol. 102, pp. 13-30, 2015.
[<http://dx.doi.org/10.1016/j.engstruct.2015.08.013>]
- [29] *GB50010-2010, Code for Design of Concrete Structures*, China Architecture & Building Press: Beijing, 2010. Available at : <https://www.scribd.com/doc/213112492/GB-50010-2010-%E6%B7%B7%E5%87%9D%E5%9C%9F%E7%BB%93%E6%9E%84%E8%AE%BE%E8%AE%A1%E8%A7%84%E8%8C%83-%E5%90%AB%E6%9D%A1%E6%96%87%E8%AF%B4%E6%98%8E>
- [30] J.B. Mander, M.J. Priestley, and R. Park, "Theoretical stress-strain model for confined concrete", *Journal of Structural Engineering*, vol. 114, pp. 1804-1826, 1988.
[[http://dx.doi.org/10.1061/\(ASCE\)0733-9445\(1988\)114:8\(1804\)](http://dx.doi.org/10.1061/(ASCE)0733-9445(1988)114:8(1804))]
- [31] E. Brunesi, R. Nascimbene, F. Parisi, and N. Augenti, "Progressive collapse fragility of reinforced concrete framed structures through incremental dynamic analysis", *Engineering Structures*, vol. 104, pp. 65-79, 2015.
[<http://dx.doi.org/10.1016/j.engstruct.2015.09.024>]
- [32] F.J. Vecchio, and M.P. Collins, "Compression response of cracked reinforced concrete", *Journal of Structural Engineering*, vol. 119, pp. 3590-3610, 1993.

[[http://dx.doi.org/10.1061/\(ASCE\)0733-9445\(1993\)119:12\(3590\)](http://dx.doi.org/10.1061/(ASCE)0733-9445(1993)119:12(3590))]

- [33] M. Bruggi, and P. Duysinx, "Topology optimization for minimum weight with compliance and stress constraints", *Structural and Multidisciplinary Optimization*, vol. 46, pp. 369-384, 2012.
[<http://dx.doi.org/10.1007/s00158-012-0759-7>]
- [34] Z. Bolong, *Seismic Test of Structure.*, Seismological Press: Mexico, 1989.
- [35] E. Brunesi, R. Nascimbene, D. Bolognini, and D. Bellotti, "Experimental investigation of the cyclic response of reinforced precast concrete framed structures", *PCI Journal.*, 2015.
[<http://dx.doi.org/10.15554/pcij.03012015.57.79>]

© Lai *et al.*; Licensee Bentham Open.

This is an open access article licensed under the terms of the Creative Commons Attribution-Non-Commercial 4.0 International Public License (CC BY-NC 4.0) (<https://creativecommons.org/licenses/by-nc/4.0/legalcode>), which permits unrestricted, non-commercial use, distribution and reproduction in any medium, provided the work is properly cited.